

# Windbreak Effectiveness for Storage Pile Fugitive Dust Control: A Wind Tunnel Study

**B. J. Billman Stunder**

National Oceanic and Atmospheric Administration  
Silver Spring, Maryland

**S. P. S. Arya**

North Carolina State University  
Raleigh, North Carolina

Results of wind tunnel experiments to determine the optimal size and location of porous windbreaks for controlling fugitive dust emissions from storage piles in a simulated neutral atmospheric boundary layer are presented. Straight sections of windbreak material were placed upwind of two nonerodible, typically shaped piles and were also placed on the top of one of the piles. Wind speed near the pile surface is considered here as the primary factor affecting particle uptake. Wind speed distributions about the piles with and without porous windbreaks are presented. Relative wind speed reduction factors are described and efficiencies based on the relationship between wind speed and particle uptake are given. The largest and most solid windbreak caused the greatest wind speed reduction, but similar wind speed reductions were also obtained from several smaller windbreaks. A 50 percent porous windbreak of height equal to the pile height and length equal to the pile length at the base, located one pile height from the base of the pile was found to be quite effective in reducing wind speeds over much of the pile. Windbreaks placed on the top of a flat-topped pile caused large wind speed reductions on the pile top, but small, if any, reductions on the windward pile face. Windbreak effectiveness decreased as the angle between the windbreak and the wind direction decreased.

Fugitive dust from sources such as storage piles, materials transfer points, unpaved roads, and agricultural tilling contribute significantly to total suspended particulate (TSP) levels in some regions of the country. In addition to limits on ambient concentrations of TSP, radioactive particulate is also regulated. Early air pollution control efforts emphasized controlling emissions from stacks rather than fugitive dust emissions because the greater bulk of pollutants of concern at that time came from stacks. Now, control methods for fugitive dust emissions are also being tested. This wind tunnel study of windbreak effectiveness for the control of fugitive dust from storage piles was undertaken for the EPA Air and Energy Engineering Research Laboratory as part of our cooperative agreement with the U.S. EPA.

Storage pile fugitive dust emission rates depend upon the stored material's bulk density, moisture content and particle size distribution, the storage pile geometry, the wind velocity

near the pile surface and other parameters. However, particle uptake does not occur unless the wind speed is greater than a threshold velocity, which is dependent upon the type of stored material, its moisture content and particle size distribution. Several empirical relationships between wind speed and particle uptake rate are found in the literature. Storage pile emission rates have been shown to be related linearly to wind speed,<sup>1</sup> or to the cube of wind speed.<sup>2</sup> Gillette<sup>3</sup> has suggested that friction velocity, rather than wind speed, is important. Field tests have indicated that threshold friction velocities range from 0.2 to 2 m/s depending upon the type of material.<sup>4-6</sup> In other field tests, threshold wind speeds of about 10 m/s at a height of 15 cm above a coal pile surface were estimated<sup>7,8</sup> and implied that very strong winds are needed for erosion to commence. A more comprehensive review of storage pile wind erosion emission factors is given by Currier and Neal.<sup>9</sup>

The use of windbreaks for storage-pile fugitive-dust control is based upon the existence of a sheltered region downstream of a windbreak. Wind tunnel and field experiments have shown that windbreaks produce large areas of reduced wind speed in their lee.<sup>10</sup> Recirculation regions are evident both upwind and downwind of a solid windbreak; they are regions of low velocity and high turbulence intensity. Air incident on a porous windbreak flows over, around, and through the windbreak, but regions of reduced wind speed occur both downwind and upwind.<sup>11,12</sup> Greater wind speed reductions and turbulence intensity ( $u'/U$ , where  $u'$  is the r.m.s. longitudinal velocity fluctuation and  $U$  is the mean wind speed) enhancements occur with decreasing porosity.<sup>11</sup> The maximum in  $u'$  is located just above and extends downstream from the top of the windbreak, as a result of turbulence generated in the windbreak-induced shear layer. As expected, the location of the sheltered region shifts as the wind direction varies from that of the windbreak normal.<sup>13-15</sup> Measurements along the windbreak normal show that the minimum wind speed increases and its location moves toward the windbreak as the angle between the wind direction and the windbreak normal increases.<sup>14</sup>

Very little information on the use of windbreaks as a storage pile fugitive dust control method is contained in the literature. Low efficiencies were reported by Bohn *et al.*<sup>16</sup> and Jutze *et al.*<sup>17</sup> although these were only estimates. No guidelines on windbreak design and use are available. Results of a water flume study indicated that the windbreak

Copyright 1988—APCA

height should be at least  $1.4H$ , where  $H$  is the pile height, and that the lower two-thirds of the windbreak be 20 percent porous and the remainder, 50 percent porous.<sup>18</sup> However, the author did not state whether more than one windbreak height and porosity were used, nor were details of windbreak length and location, relative to the pile, and the simulated boundary layer given. Results from a wind tunnel study using a two-dimensional windbreak and pile are reported by Soo *et al.*<sup>19</sup> and Cai *et al.*<sup>20</sup> Combinations of two windbreak heights, two porosities, and five positions were tested. Optimal windbreak location was found to depend on both the windbreak height and porosity. The lower porosity windbreak caused lower wind speeds.

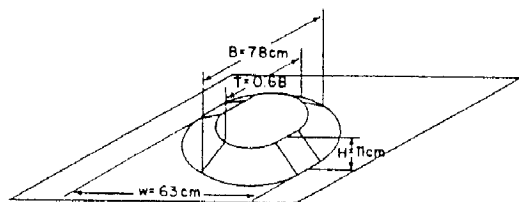


Figure 1. Sketch of the model oval, flat-topped pile.

In the present study, surface wind speed is isolated as the primary factor affecting particle uptake, although moisture content, particle size, and bulk density affect fugitive dust emissions as well. Wind speed was measured near the pile surface with and without windbreaks of several sizes and porosities located at various distances upwind or on the top of the two typically shaped storage piles. No effort was made to simulate fugitive dust emissions. Effect of wind direction is also studied. The observed wind speed patterns are used to determine the optimal windbreak porosity, height, length, and location, and to develop windbreak design guidelines for storage pile fugitive dust control. A more detailed description of experiments and results is given elsewhere.<sup>21</sup>

## Experimental Arrangement and Instrumentation

### Modeling Approach

The experiment was conducted in the EPA Meteorological Wind Tunnel (MWT), a low-speed, open-return tunnel having a test section 2.1 m high  $\times$  3.7 m wide  $\times$  18.3 m long. A complete description of the MWT and operating characteristics are given by Snyder.<sup>22</sup> Simulating the lower part of the atmospheric boundary layer (ABL) during strong winds

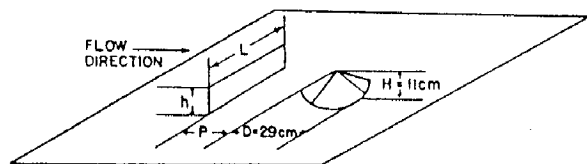


Figure 2. Sketch of the model conical pile and windbreak.

(wind speed exceeding the threshold value) and determining model size and shape are necessary to assure that wind tunnel results will be valid for the full-scale case under investigation. The neutrally stratified simulated boundary layer was characterized by a depth of approximately 1 m, roughness length ( $z_0$ ) of 0.12 mm, and friction velocity ( $u^*$ ) of  $0.048U_0$ , where  $U_0 = 4$  m/s is the free-stream speed. Details of the simulated boundary layer are given by Castro and Snyder.<sup>23</sup>

Model size and free-stream wind speed should ideally be determined from matching the model and full-scale Reynolds numbers ( $Re$ ). However, the requirement of matching  $Re$  can be relaxed, if the Reynolds number of the simulated flow exceeds a certain minimum (critical) value around  $10^4$ , above which the mean flow and large-eddy structures become essentially independent of  $Re$ .<sup>24</sup> With our simulated  $Re \approx 3 \times 10^4$ , based on an ambient air speed of 4 m/s and the model pile height of 0.11 m, we can expect the concept of Reynolds number independence to be valid. Hence wind tunnel velocities, normalized by an appropriate scaling velocity, are equivalent to normalized full-scale values, provided the relevant length scale ratios are matched for geometric similarity.

No two storage piles have the same shape and size, and active piles have constantly changing dimensions. For purposes of the present study, windbreak effects on two typical, but idealized, pile geometries are studied; the results may be applicable to similar full-scale piles. Based on a survey of coal pile shapes at several electric generating plants, the two piles modeled had the same height (11 m) and side slopes ( $37^\circ$ ), but different shapes, one a cone and the other an oval, flat-topped pile, as shown in Figures 1 and 2. Since typical pile and windbreak heights are well within the surface layer (lowest 100 m of the neutrally stratified atmosphere<sup>25</sup>), matching the ratio of the pile height to the boundary layer

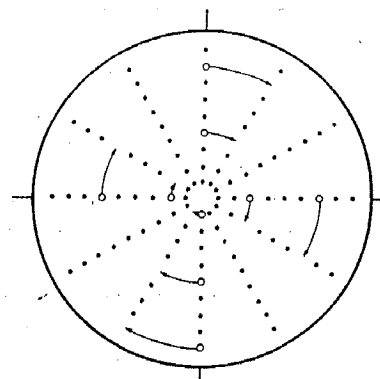


Figure 3. Top view of conical pile. Circles: thermistor positions on pile. Dots: effective thermistor positions due to pile rotation.

depth was not considered important. Instead, Jensen's<sup>26</sup> criterion of matching the ratio of the pile height to the surface roughness length was used to obtain the scaling ratio between the model and prototype of 1:100. The model surfaces were roughened with a 4 mm size gravel which satisfied the criterion for aerodynamically rough surfaces.<sup>27</sup>

The windbreak and conical pile set-up is shown in Figure 2. Windbreaks were constructed of synthetic material of 50 percent porosity that is commercially available for windbreak use and a nylon mesh screen of 65 percent porosity. Windbreaks of two porosities, heights  $0.5H$ ,  $1.0H$ , and  $1.5H$ , where  $H$  is the pile height; and lengths  $1.0D$  and  $1.5D$ , where  $D$  is pile base diameter, were placed at distances of  $1H$  and  $3H$  from the upstream pile base, resulting in a total of 24 cases that were tested. One windbreak was also placed at angles of  $20^\circ$  and  $40^\circ$  from the position normal to the incident flow.

For the oval, flat-topped pile, one of the windbreak orientations was similar to that shown in Figure 2 with the longer axis of the pile being parallel to the windbreak. The same windbreak porosities, relative sizes and positions were used (the windbreak length is given in terms of the pile base length  $B$ ) although not all of the 24 possible combinations were tested. Additional tests were conducted with windbreak heights  $0.75H$  and  $1.25H$ , and length 0.6 times the pile

base length. The other windbreak locations tested were on the pile top, either close to the centerline or at the upstream edge of the pile top parallel to the pile's longer axis. Two heights,  $0.14H$  and  $0.27H$ , and two lengths,  $0.16T$  and  $0.5T$ , where  $T$  is the pile top length, were tested. For windbreaks in both positions the pile was rotated  $20^\circ$  and  $40^\circ$  to simulate other wind directions.

An additional phase of the study was to measure mean velocity and turbulence intensities downstream of the less porous windbreak oriented normal to the air flow to determine whether reverse flow was present and to determine the regions of reduced mean flow and enhanced turbulence. The windbreak chosen was 50 percent porous, 112 mm high and 1180 mm long (aspect ratio 10.5).

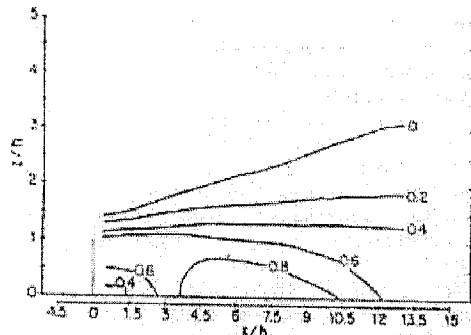


Figure 4. Relative wind speed reductions downstream of a porous windbreak.

#### Instrumentation

Velocity profiles were measured at selected locations over the flat tunnel floor and downstream of a windbreak with hot-wire and pulsed-wire anemometers that were mounted on the instrument carriage in the wind tunnel.<sup>21</sup> Wind speeds were measured at a number of points over and close to the pile surface with heated thermistors. Physical characteristics and measurement techniques of the three anemometers are briefly discussed in the following.

A hot-wire anemometer (HWA) was used to obtain vertical profiles in the undisturbed (no pile, no windbreak) boundary layer and downstream of a windbreak. Mean velocity, angle of flow, and several turbulence quantities were obtained using the conventional hot-wire technique with frequent calibrations and the yaw response corrections developed by Lawson and Britter.<sup>28</sup> The hot-wire output was digitized and processed at a rate of 500 Hz. A sampling time of 90 s provided reasonably repeatable results.

A pulsed-wire anemometer (PWA) was used to measure mean flow and turbulence intensity downstream of a windbreak since flow visualization indicated intermittent flow reversal. The PWA senses both wind speed and direction. Details on the theory of the PWA and its operation are given by Bradbury and Castro<sup>29</sup> and Castro and Snyder.<sup>23</sup> A sampling rate of the 20 Hz and sampling time of 3 minutes gave reasonably repeatable results.

It is difficult to measure the wind speed near the rough, sloping surface of the pile, particularly when the wind direction at the measurement point is unknown and difficult to determine. Pitot-static tubes and hot-wire anemometers require certain orientation with respect to the wind for accurate results and cannot be readily used to measure the wind or stress field over the whole pile surface. Heated thermistors projecting out of the pile surface were found to be more suitable and economical for this purpose. Fenwal thermistors of 1 mm bead diameter and 1.5 mm length, with a time constant of 4 s in still air at  $25^\circ\text{C}$  were used. The electric

circuit consisted of a regulated power supply of constant voltage  $E$  and thermistor-resistor pairs in parallel with the power supply. The voltage across each series resistor was the output voltage which was digitized at a rate of 50 Hz. A one-minute sampling time was found to be adequate.

Thermistor anemometers operate under the same basic principle as do hot-wire anemometers, that is, the heat loss from the sensor is a function of wind speed. Rasmussen<sup>30</sup> has shown that

$$i^2 R = K(T_t - T_a) \quad (1)$$

where  $i$  is current through the thermistor,  $R$  is thermistor resistance,  $T_t$  and  $T_a$  are thermistor and ambient temperature, respectively, and  $K$  is the dissipation factor.  $K$  is a function of the wind speed and the properties of the fluid surrounding the thermistor, and was determined experimentally from calibration in a small wind tunnel as

$$K = 0.97u^{0.27} \quad (2)$$

where  $u$  is in  $\text{m s}^{-1}$  and  $K$  is in  $\text{mW } ^\circ\text{C}^{-1}$ .

Nine thermistors were mounted at different elevations on the conical pile in the arrangement shown in Figure 3. The thermistors were mounted normal to and about 2 to 3 mm above the pile surfaces. Close to the surface the flow presumably parallels the surface and wind speed may be assumed to be directly related to the surface shear stress. Each run consisted of measuring the wind speed with the nine thermistors, rotating the pile  $30^\circ$ , measuring the wind speed at these nine positions, etc., through  $360^\circ$ , resulting in 108 data points per run. Eighty-one thermistors were mounted in a regular pattern over the entire surface of the oval, flat-topped pile. Each run consisted of measuring the wind speed at the 81 positions for one pile orientation.

Possible systematic errors resulting from the application of the same calibration curve (Equation 2) to all the thermistors, effects of individual roughness elements and the variable thermistor height above the surface could be as large as 20 percent if absolute wind speeds are desired. In the present study, however, our interest was more in relative wind speeds over the pile surface, such as the ratio of wind speeds with and without a windbreak or with two different windbreaks. Errors in relative wind speed are estimated to be less than 10 percent.

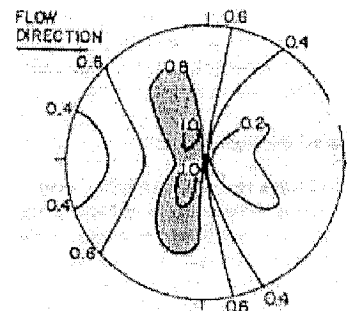


Figure 5. Normalized surface wind speed ( $u/u_0$ ) about the conical pile for no windbreak case.

#### Flow about a Porous Windbreak

The porous windbreak caused a large area of reduced wind speed in its lee. Relative wind speed reduction due to a windbreak may be defined as  $[U_R(z) - U(z)]/U_R(z)$ , where  $U_R(z)$  is the reference speed (measured with the HWA) at the location of the windbreak but in its absence, and  $U(z)$  is a speed (measured with the PWA) at some distance down-

stream of the windbreak. Lines of constant speed reductions are shown in Figure 4. Downstream distance and height are scaled by the windbreak height  $h$ . Below  $z = 1h$ , wind speeds were reduced at least 50 percent from the upstream value at the same height. The greatest reductions were observed for heights less than  $z = 0.5h$  between approximately  $4h$  and  $8h$  downstream. Flow visualization indicated intermittent flow reversal near the surface in this region. Note that the maximum reduction of wind speed did not occur immediately downstream of the windbreak, but occurred farther downstream. A strong gradient is clearly evident just above and downstream of the windbreak.

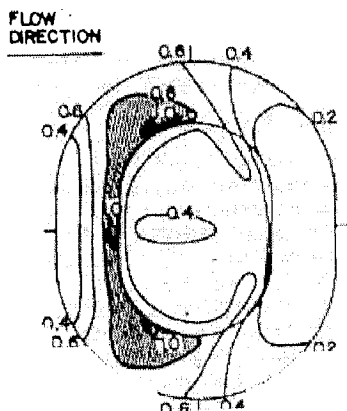


Figure 6. Normalized surface wind speed ( $u/u_i$ ) about the oval, flat-topped pile for no windbreak case.

The pattern of turbulence intensity downstream of a windbreak was similar to that of wind speed reduction. Turbulence intensity is the ratio of the r.m.s. fluctuating longitudinal velocity  $u'$  at a given location to the mean wind speed at that location. Intensities of greater than 30 percent were observed for heights less than  $1.5h$ , between  $x = 2h$  and  $12h$ . The maximum in  $u'$  occurred between  $z \approx 1.25h$  and  $1.5h$  which suggests that greater turbulence is generated in the shear layer separating from the top of the windbreak.

The observed flow structure downwind of a porous windbreak was qualitatively similar to that observed by Raine and Stevenson,<sup>11</sup> but there are quantitative differences due to differences in the windbreaks and simulated boundary layer characteristics in the two studies.

#### Flow about Simulated Storage Piles

It is important to locate the areas of high wind speed near the pile surface in the absence of a windbreak since that is where particle uptake is most likely to occur. Similarly, the areas where wind erosion is least likely to occur are those with low wind speed. Figures 5 and 6 show the top views of the conical and oval, flat-topped piles, respectively, with contours of normalized wind speed,  $u/u_i$ , where  $u$  is the wind speed at the pile surface measured with the thermistor and  $u_i$  is the wind speed at the equivalent full-scale height of 10 m in the absence of the pile. Ten meters was chosen as the reference height rather than 11 m, the pile height, because the former is the standard height to which "surface" wind speed measurements are usually referenced in the meteorological literature. Note that the air flow in the figure is from the left. Correction factors for the thermistors on the flat-topped pile were developed based upon the data from the  $0^\circ$  and  $180^\circ$  pile orientations, assuming flow symmetry around the pile surface; these were used in subsequent measurements. For both piles the areas of maximum wind speed were

near the top on the upwind sloping faces and extended toward the sides of the pile. The maximum normalized speed ( $u_{max}/u_i$ ) was 1.16 and 1.12 for the conical and flat-topped piles respectively. The areas of minimum wind speed are in the lee of piles and on the top of the flat-topped pile. High speeds along the pile sides are expected because the flow is accelerated in going around the pile. The flow separates on the lee side, resulting in a region of low-speed recirculating flow.

#### Windbreak Effects on Flow About Storage Piles

Effects of windbreak height, length, porosity and position on wind speed about the pile are discussed for the case of a windbreak placed upstream of both the piles and on the top of the flat-topped pile. Effect of wind direction was also studied. Relative wind speed reduction and the observed maximum wind speed were used to assess the relative effectiveness of various windbreaks.

Initial guidance on the desired size of the windbreak and its location was obtained from an examination of the observed flow and sheltered region behind the windbreak in the absence of the pile. Since height and width of the sheltered region are directly related to windbreak height and length, windbreaks placed upstream of the pile having dimensions less than the pile height or length are expected to be less efficient.

With a windbreak, the wind speed at a given location on the pile surface is some fraction of that in the unprotected case. The relative amount by which the wind speed is reduced is called the wind speed reduction factor  $R_i$  and, in percent, is defined as

$$R_i = (u_{0,i} - u_i)/u_{0,i} \times 100, \quad (3)$$

where  $u_i$  and  $u_{0,i}$  are wind speeds at the  $i$ th location on the pile for the cases with and without the windbreak, respectively.

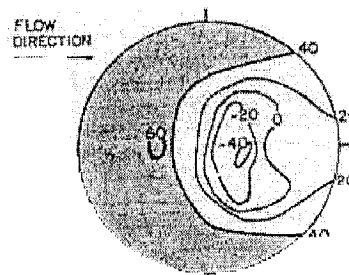


Figure 7. Wind speed reduction factor ( $R_i$ , %) for the 65 percent porous windbreak of height  $0.5H$  and length  $1.0D$  placed  $1H$  from the conical pile base.

tively.  $R_i$  is zero when the windbreak causes no change in the wind speed, and 100 percent when the wind speed is reduced to zero. It is important to remember that the combined effects of windbreak height, length, porosity, and position, as well as turbulence in the approach flow, and pile shape, size and surface roughness determine the wind speed distribution over the pile surface. Some of these factors will be considered here. First, the cases of windbreaks normal to the air flow are discussed.

An optimum windbreak size (height and length) exists since a very small windbreak is expected to be ineffective and a very large windbreak may be effective in reducing wind speeds but may turn out to be too expensive. Contours of constant wind speed reduction factor  $R_i$  resulting from 65 percent porous screen of height  $0.5H$ , located a distance  $H$  from the pile base and length  $1.0D$  for the conical pile (Fig-

ure 7) and  $1.0B$  for the oval pile (Figure 8) are shown. Referring also to Figures 5 and 6, in the areas of maximum wind speed without the windbreak, these windbreaks reduced the wind speed by 20 to 30 percent. For both piles, relatively large wind speed reductions occurred in the lower portion of the upstream face, with the greatest reductions apparent near the piles' centerlines. Regions of wind speed increase (negative reduction factor) were observed on the lee side of the conical pile and on the top, upstream-half of the larger pile. The increase in speed observed on the top of the larger pile may be due to a combination of air deflection about the windbreak and the pile. In terms of fugitive dust control, these increases are probably not significant for the conical

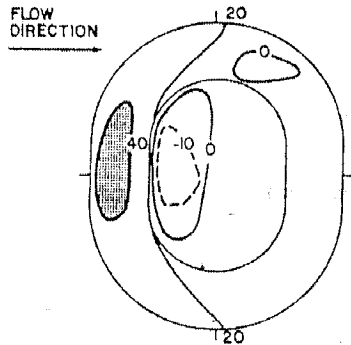


Figure 8. Wind speed reduction factor ( $R_i$  %) for the 65 percent porous windbreak of height  $0.5H$  and length  $1.0B$  placed  $1H$  from the oval, flat-topped pile base.

pile because the wind speeds will be relatively low in this region unless the reference speed ( $u_r$ ) is very high, but the increase could be significant for the larger pile, again depending on  $u_r$ . This general pattern of wind speed reduction was typical of all the windbreaks of height  $0.5H$ , but not of the higher windbreaks.

For higher windbreaks (heights  $1.0H$  and  $1.5H$ ) upstream of the conical pile, the area of greatest wind speed reduction was the upper part of the windward side, with typical reductions of at least 50 percent (see Figure 9). Areas of negative reduction factors (up to  $\approx -15$  percent) were observed only with windbreaks of height  $1.0H$  located  $3H$  from the conical pile; these areas were significantly smaller than those observed with lower windbreaks (Figure 7). Wind speeds were reduced everywhere for the other higher windbreak with reduction factors ranging up to 90 percent. In general, the reduction pattern for windbreaks of the same porosity, length, and position did not differ significantly when the windbreak height was increased from  $1.0H$  to  $1.5H$ . Figure 9 shows the effect of increased porosity on windbreak effectiveness.

For higher windbreaks (heights  $1.0H$  and  $1.5H$ ) upstream of the oval, flat-topped pile, wind speeds were reduced everywhere (see Figure 10). Increasing the height from  $1.0H$  to  $1.5H$  gave greater reductions on the pile top, but the general pattern of wind speed reduction depended upon the windbreak location. In general, a windbreak of height  $1.0H$  located a distance  $1H$  upwind of the pile base gave similar wind speed reductions (30–60 percent) on the top part of the upstream face and on the pile top. Increasing the height to  $1.5H$  caused greater reductions (40–80 percent) only on the pile top. A windbreak of height  $1.0H$  in the  $3H$  position caused higher reductions on the upstream face (45–75 percent) than on the pile top (10–45 percent).

Length of the windbreak relative to the pile dimension across the flow is also an important parameter. Wind speed reductions up to 40 percent were observed on both sides of

the flat-topped pile with windbreaks of length  $0.6B$  which is equal to the maximum length of the flat-topped pile at the top. Longer windbreaks (length =  $1.0B$ ) caused much higher reductions in wind speeds (at least 60 percent) at the sides of the flat pile top (Figure 10). Increasing the windbreak length beyond the pile base length ( $B$ ) did not significantly alter the wind speed reductions. Length becomes more important, however, if the incident wind is not normal to the windbreak (see later discussion).

The effect of the distance between the windbreak and pile on wind speed reduction appears to be related to windbreak height. In general, windbreaks of height  $0.5H$  caused greater wind speed reduction in the lower part of the windward face and toward the sides when placed a distance equal to the pile height ( $1H$ ) rather than a distance three times the pile height ( $3H$ ) from the piles' bases. Windbreaks of height  $1.5H$  placed  $3H$  from either pile caused greater wind speed reductions on the windward face than if the windbreak were at the  $1H$  position. Both locations were found to be equally effective for windbreaks of height  $1.0H$ .

Patterns of wind speed reduction factors clearly show effects of windbreak height, length, porosity and position. The maximum wind speed measured by a thermistor on the pile, independent of position, may also be used to assess relative effectiveness of the various windbreaks since it is related to the maximum particle emission rate. Values of maximum wind speed  $u_{max}$  normalized by the wind speed  $u_r$  at the equivalent full-scale height of 10 m in the absence of the pile for the windbreaks normal to the flow are given in Tables I and II for the conical and oval, flat-topped piles, respectively. Recall that the ratio  $u_{max}/u_r$  is 1.16 and 1.12 for the unprotected (no windbreak) cases. In general, higher maximum wind speeds are observed for windbreaks upstream of the oval, flat-topped pile than for the corresponding windbreak with the conical pile, although their trends with increasing windbreak height are similar for both piles.

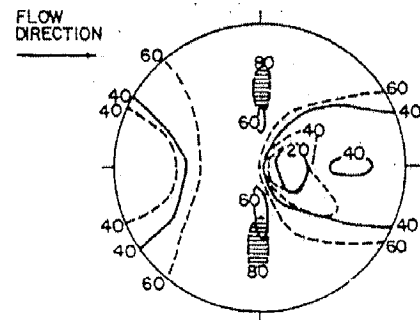


Figure 9. Wind speed reduction factor ( $R_i$  %) for the windbreak of height  $1.0H$  and length  $1.0D$  placed  $1H$  from the conical pile base with porosity 65 percent (solid line) and 50 percent (dashed line).

All the windbreaks reduced maximum wind speed. Windbreaks of height  $0.5H$  gave much higher  $u_{max}/u_r$  than did the higher windbreaks. Differences in  $u_{max}/u_r$  between windbreaks of height  $1.0H$  and  $1.5H$ , for the same porosity, length, and position, were not nearly as great as for those between  $0.5H$  and  $1.0H$ . In general, for a given windbreak height, length, and position, the 50 percent porous windbreak caused lower  $u_{max}/u_r$  than did the 65 percent porous windbreak. Windbreaks shorter than the length of the pile base were clearly less effective. Optimum location depends on the windbreak height and length.

The effect of changes in wind direction from the normal to the windbreak was studied for the 50 percent porous windbreak of height  $1.0H$ , length  $1.0D$ , placed a distance  $1H$  from

the conical pile base. The ratio  $u_{max}/u_r$  was 0.31, 0.69, and 1.12 for the cases with angles of 0°, 20°, and 40° between the incident wind and the windbreak normal, respectively. For the 0° case wind speed reductions were at least 40 percent over much of the pile. For the 20° case, a region of much lower reductions was observed on the side of the pile opposite the windbreak, indicating that the windbreak length and position are important. For the 40° case, the region of reductions greater than 40 percent was quite small; indeed wind speed increases were observed. Clearly, windbreak effectiveness decreases with increasing angle of flow from the normal.

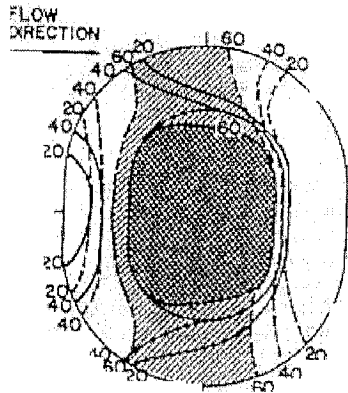


Figure 10. Wind speed reduction factor ( $R_i$ , %) for the 50 percent porous windbreak of height  $1.5H$  placed  $1H$  from the oval, flat-topped pile base with length  $0.6B$  (solid line) and  $1.0B$  (dashed line).

Our results for the windbreak-protected piles may be compared with two previous laboratory studies in which windbreaks were located upwind of a pile. Davies<sup>18</sup> recommended a windbreak height of  $1.4H$ , which is consistent with our results. But he did not report the detailed results of the various cases tested, which could be compared to ours. The present work has extended the studies by Soo *et al.*<sup>19</sup> and Cai *et al.*<sup>20</sup> by using three-dimensional piles and windbreaks of different heights and porosities. In both the previous studies, optimal windbreak location was found to be related to the windbreak height, and lower wind speeds were observed with less porous windbreaks.

In addition to placing windbreaks upstream of both piles, some were placed on the top of the oval, flat-topped pile. Large wind speed reduction factors (up to 65 percent) on the pile top were observed for all the cases. The location and extent of the area with significant wind speed reduction depended upon windbreak size, location, and angle of the incident flow. The area of coverage and magnitude of the wind speed reductions were greater for a higher windbreak. Similarly, longer windbreaks caused larger sheltered regions, which were confined, however, to the pile top. The greatest reductions were observed in areas between about  $3h$  and  $6h$  downstream of the windbreak. A windbreak placed near the centerline of the pile caused wind speed reductions downstream and, to a lesser extent, upstream of the windbreak on the pile top. Reduction factors for a windbreak placed near the centerline of the pile with the incident flow 40° to the windbreak normal showed that the sheltered area shifted with the wind direction. These results suggest that fugitive dust emissions on the top of the pile may be controlled locally through the use of a windbreak at the top of the pile.

#### Windbreak Efficiency for Fugitive Dust Control

Windbreak effectiveness in controlling fugitive dust emissions from storage piles may be assessed by several methods. Wind speed reduction patterns and the normalized maximum wind speed have already been described. Further analyses based on particle uptake at wind speeds exceeding a given threshold value will be described.

In terms of fugitive dust emissions, the windbreak efficiency  $E$  may be defined as

$$E = 1 - (Q/Q_0) \quad (4)$$

where  $Q$  and  $Q_0$  are the storage pile fugitive dust emission rates with and without the windbreak, respectively. Since only surface wind speeds have been measured here, assumed relationships between wind speed and emissions are used to calculate efficiencies. A windbreak may reduce wind speeds to values less than the threshold for particle uptake over part or all of the pile. Hence a better definition of efficiency would include a threshold value. However, threshold speeds have been determined only for a few cases as discussed earlier. The relationship between threshold speed and particle size and moisture content is not well understood. To a first approximation, it is assumed here that the reference wind speed is sufficiently high, so that wind speeds everywhere, with and without a windbreak, exceed the threshold.

Table I.  $u_{max}/u_r$  for the various windbreaks placed upstream of the conical pile

Height	Position: Length:	65% porous windbreak				50% porous windbreak			
		1H		3H		1H		3H	
		1.0D	1.5D	1.0D	1.5D	1.0D	1.5D	1.0D	1.5D
		0.91	0.93	0.91	0.94	0.90	0.93	0.82	0.86
		0.55	0.59	0.54	0.56	0.31	0.34	0.37	0.27
		0.56	0.60	0.50	0.52	0.39	0.42	0.25	0.17

Table II.  $u_{max}/u_r$  for the various windbreaks placed upstream of the oval, flat-topped pile.

Height	Position: Length:	65% porous windbreak				50% porous windbreak			
		1H		3H		1H		3H	
		0.6B	1.0B	0.6B	1.0B	0.6B	1.0B	0.6B	1.0B
		0.98	0.96	0.97		0.95	0.92	0.93	0.87
							0.58		0.66
		0.85	0.70	0.84	0.68	0.73	0.45	0.78	0.56
							0.48		0.36
		0.78	0.69	0.79		0.63	0.45	0.66	0.28

Table III. Efficiency ( $E_1$ ) for the various windbreaks placed upstream of the conical pile.

Height	Position: Length:	65% porous windbreak				50% porous windbreak			
		1H		3H		1H		3H	
		1.0D	1.5D	1.0D	1.5D	1.0D	1.5D	1.0D	1.5D
0.5H		34	32	28	30	46	45	36	36
1.0H		48	45	53	52	66	67	65	71
1.5H		46	44	55	54	64	65	71	77

Table IV. Efficiency ( $E_1$ ) for the various windbreaks placed upstream of the oval, flat-topped pile.

Height	Position: Length:	65% porous windbreak				50% porous windbreak			
		1H		3H		1H		3H	
		0.6B	1.0B	0.6B	1.0B	0.6B	1.0B	1.5B	0.6B 3H 1.0B
0.5H		15	16	13	—	18	20	21	15 17
0.75H		—	—	—	—	—	41	—	— 34
1.0H		27	34	28	37	34	53	51	31 49
1.25H		—	—	—	—	—	56	—	— 57
1.5H		33	39	38	—	44	58	59	43 62

Then a percentage efficiency can be defined based upon a given power law relation,  $Q\alpha u^n$  (where  $n$  is between 1 and 3), between wind speed and particle uptake.

$$E_n = \left[ 1 - \frac{\sum (u_i^n A_i)}{\sum (u_{0,i}^n A_i)} \right] \times 100, \quad (5)$$

where the summation is over the entire pile. In effect, these efficiencies are  $1 - (\bar{u}^n / \bar{u}_0^n)$ , where  $\bar{u}^n$  and  $\bar{u}_0^n$  are the area-averaged values over the pile surface with and without a windbreak, respectively. Efficiencies  $E_1$  and  $E_3$  are calculated here, using values of  $n = 1$  and 3. The above definition of the efficiency differs from that used by Billman.<sup>31</sup>

Efficiencies ( $E_1$ ) for the windbreaks placed upstream of the conical and oval, flat-topped piles with normal incident flow are given in Tables III and IV, respectively. In general, a windbreak is more effective (higher  $E_1$ ) when placed upstream of the conical pile, as compared to a windbreak of the same relative size placed upstream of the larger, oval-shaped pile. Trends in  $E_1$  with changes in height, length, location and porosity of the windbreak are similar for both piles. In general, a windbreak at least as high as the pile is desirable. The 1.5H height was slightly more effective than the 1.0H height with the oval, flat-topped pile, reflecting increased wind speed reductions on the pile top for the highest wind-

break. Efficiencies are higher for the less porous windbreak material. Except for the windbreaks of height one-half the pile height (0.5H), efficiency is lower when the windbreak is not as long as the pile base length.

Trends in the values of  $E_3$ , (the efficiency based upon the  $u^3$  relation to dust uptake) with windbreak height, length, location and porosity are found to be similar to those for  $E_1$ , except the values of  $E_3$  are considerably larger than those of  $E_1$ . The trends are clearly seen in a plot of efficiency ( $E_3$ ) vs. windbreak height as functions of windbreak length and porosity for both the piles (Figure 11).

Although the highest efficiencies of 99 percent and 96 percent correspond to the 50 percent porous material of height 1.5H, length 1.5D or 1.0B, located 3H from the base of both the piles, the efficiencies of the more economical windbreak of the same porosity, height equal to the pile height and length equal to the pile base length are only slightly lower (97 percent and 89 percent, respectively). Clearly, the latter size would be preferable on the basis of cost effectiveness. Any location between 1H and 3H from the base of the pile could be chosen depending on the convenience.

Windbreak efficiencies presented here are generally much higher than those estimated by Bohn *et al.*<sup>16</sup> and Jutze *et al.*<sup>17</sup> indicating that windbreaks may be a highly effective fugitive-dust control method.

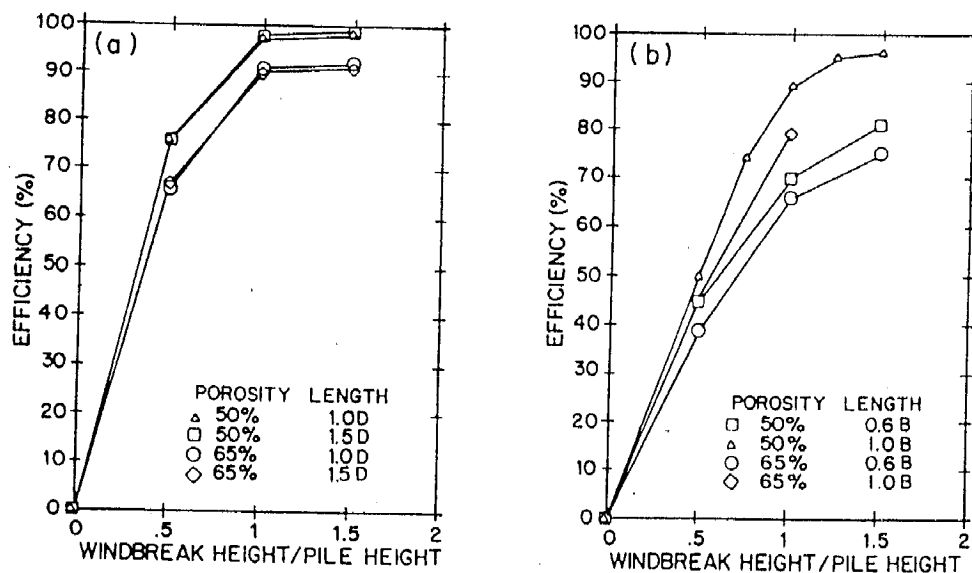


Figure 11. Efficiency ( $E_3$ ) vs. height for windbreaks placed 3H from the pile base: (a) conical pile, (b) oval, flat-topped pile.

## Conclusions

This wind tunnel study has shown that windbreaks normal to the wind direction placed upwind of a conical and larger, oval, flat-topped storage pile can significantly reduce wind speed near the surface of the pile, and hence, fugitive dust emissions. Of the windbreaks tested for each pile, the largest 50 percent porous windbreak placed  $3H$  from the pile appears to be the best in terms of greatest wind speed reductions and effectiveness for fugitive dust control. However, all the 50 percent porous windbreaks at least as high as the pile and as long as the pile base had similar overall effects. Windbreaks of height and/or length less than that of the pile were clearly less effective. Optimal windbreak location appears to be related to windbreak height, particularly for the conical pile; the higher the windbreak, the farther it should be located upwind of the pile. However, locations farther than  $3H$  were not examined.

Windbreak length and position are even more important in determining effectiveness when the air flow is not normal to a windbreak. With a windbreak of height and length equal to the pile height and base length, substantial wind speed reductions resulted when the windbreak was placed upwind normal to the flow and also at an angle of  $20^\circ$  to the normal, but very little reduction occurred at an angle of  $40^\circ$ .

Windbreaks placed on the top of the oval, flat-topped pile caused large areas of significant wind speed reductions on the pile top both downwind and upwind of the windbreak, but very small reductions to the high wind speeds on the windward face occurring in the absence of any windbreak. The area of greatest reduction was not immediately downwind of the windbreak, but displaced farther downstream. Changes in wind direction shifted the location of the sheltered region. These results suggest that fugitive dust emissions may be locally controlled with windbreaks placed on the top of a relatively level storage pile. In particular, portable windbreaks may be quite practical since they could be positioned to protect active areas of the pile.

Design guidelines developed by Soo *et al.*<sup>19</sup> and Cai *et al.*<sup>20</sup> have been extended since more windbreak configurations were examined and three-dimensional piles were used. Windbreak efficiencies are found to be much higher than previously estimated.<sup>16,17</sup> With the design guidelines presented here, the use of windbreaks for fugitive dust control appears promising.

Wind speed was isolated here as the major factor affecting storage pile fugitive dust emissions, but storage pile moisture content, type of material stored and threshold wind speed also affect emissions. A clearer understanding of the relationship of wind speed and threshold speed to fugitive dust emissions would allow for better analysis of the data presented. Additional field measurements of fugitive dust from storage piles with and without windbreaks would be helpful for comparison to the efficiencies and design guidelines presented here.

## Acknowledgments

The authors wish to acknowledge the advice and help given by Dr. W. H. Snyder and his staff at the EPA Fluid Modeling Facility. Messrs. W. B. Kuykendal and D. L. Harmon (EPA-AEERL) provided us the opportunity to work on this project. Mr. R. Lawrence (KPN, International) provided the commercial windbreak material.

This work has been supported through cooperative agreements CR-807854 and CR-811973 between North Carolina State University and the U.S. Environmental Protection Agency. It has not been subjected to the Agency's required

peer and policy review and, therefore, does not necessarily reflect the views of the Agency. No official endorsement should be inferred.

## References

1. K. Axetell, Jr., "Survey of Fugitive Dust from Coal Mines," EPA-908/1-78-003, EPA Region VIII, Office of Energy Activities, Denver, CO, February 1978.
2. T. R. Blackwood, R. A. Wachter, "Source Assessment: Coal Storage Piles," EPA-600/2-78-004k, U.S. Environmental Protection Agency, Cincinnati, OH, May 1978.
3. D. Gillette, "A wind tunnel simulation of the erosion of soil: Effect of soil texture, sandblasting, wind speed, and soil consolidation on dust production," *Atmos. Environ.* 12: 1735 (1978).
4. D. Gillette, "Tests with a portable wind tunnel for determining wind erosion threshold velocities," *Atmos. Environ.* 12: 2309 (1978).
5. D. A. Gillette, J. Adams, A. Endo, D. Smith, "Threshold velocities for input of soil particles into the air by desert solids," *J. Geophys. Res.* 85(C10): 5621, 1980.
6. C. Cowherd, Jr., R. Bohn, T. A. Cuscino, "Iron and Steel Plant Open Source Fugitive Emission Evaluation," EPA-600/2-79-103, U.S. Environmental Protection Agency, Research Triangle Park, NC, May 1979.
7. C. Cowherd, Jr., "Emission Factors for Wind Erosion of Exposed Aggregates at Surface Mines," Paper No. 82-15.5, in *Proceedings of the 75th APCA Annual Meeting*, New Orleans, LA, June 1982.
8. T. Cuscino, G. E. Muleski, C. Cowherd, Jr., "Iron and Steel Plant Open Source Fugitive Emission Evaluation," EPA-600/2-83-110, U.S. Environmental Protection Agency, Research Triangle Park, NC, October 1983.
9. E. L. Currier, B. D. Neal, "Fugitive Emissions from Coal-Fired Power Plants," EPRI CS-3455, Electric Power Research Institute, Palo Alto, CA, 1984.
10. J. Van Eimern, R. Karschon, L. A. Razumova, G. W. Robertson, *Windbreaks and Shelterbelts*, WMO Technical Note No. 59, 1964.
11. J. K. Raine, D. C. Stevenson, "Wind protection by model fences in a simulated atmospheric boundary layer," *J. Ind. Aerodyn.* 2: 159 (1977).
12. M. D. A. E. S. Perera, "Shelter behind two-dimensional solid and porous fences," *J. Ind. Aerodyn.* 8: 93 (1981).
13. J. Gandemer, "The aerodynamic characteristics of windbreaks, resulting in empirical design rules," *J. Wind Eng. Ind. Aerodyn.* 7: 15 (1981).
14. I. Seginer, "Flow around a windbreak in oblique wind," *Boundary-Layer Meteorol.* 9: 133 (1975).
15. P. J. Mulhearn, E. F. Bradley, "Secondary flows in the lee of porous shelterbelts," *Boundary-Layer Meteorol.* 12: 75 (1977).
16. R. Bohn, T. Cuscino, C. Cowherd, Jr., "Fugitive Emissions from Integrated Iron and Steel Plants," EPA-600/2-78-050, U.S. Environmental Protection Agency, Washington, DC, March 1978.
17. G. A. Jutze, J. M. Zoller, T. A. Janszen, R. S. Amick, C. E. Zimmer, R. W. Gerstle, "Technical Guidance for Control of Industrial Process Fugitive Particulate Emissions," EPA-450/3-77-010, U.S. Environmental Protection Agency, Research Triangle Park, NC, March 1977.
18. A. E. Davies, "A Physical Modelling Approach to the Solution of Fugitive Emission Problems," paper 80-68.11, in *Proceedings of the 73rd APCA Annual Meeting*, Montreal, Quebec, June 1980.
19. S. L. Soo, J. C. Perez, S. Rezakhany, "Wind Velocity Distribution over Storage Piles and Use of Barriers," in *Proceedings of the Symposium on Iron and Steel Pollution Abatement Technology for 1980*, EPA-600/9-81-017, U.S. Environmental Protection Agency, Research Triangle Park, NC, p. 85, March 1981.
20. S. Cai, F. F. Chen, S. L. Soo, "Wind penetration into a porous storage pile and use of barriers," *Environ. Sci. Technol.* 17: 298 (1983).
21. B. J. Billman, S. P. S. Arya, "Windbreak Effectiveness for Storage-Pile Fugitive-Dust Control," EPA/600/3-85/059, U.S. Environmental Protection Agency, Research Triangle Park, NC, July 1985.
22. W. H. Snyder, "The EPA Meteorological Wind Tunnel—It's Design, Construction and Operating Characteristics," EPA-600/4-79-051, U.S. Environmental Protection Agency, Research Triangle Park, NC, September 1979.
23. I. P. Castro, W. H. Snyder, "A wind tunnel study of dispersion from sources downwind of three-dimensional hills," *Atmos. Environ.* 16: 1869 (1982).